Ultraviolet and mid-infrared continuum generation by cross-phase modulation between red-shifted solitons and blue-shifted dispersive waves in a photonic crystal fiber*

Shen Xiang-Wei(申向伟)[a)†], Yuan Jin-Hui(苑金辉)[a)], Sang Xin-Zhu(桑新柱)[a)], Yu Chong-Xiu(余重秀)[a)], Rao Lan(饶 岚)[b)], Xin Xiang-Jun(忻向军)[b)], Xia Min(夏 民)[a)], Han Ying(韩 颖)[c)], Xia Chang-Ming(夏长明)[c)], and Hou Lan-Tian(侯蓝田)[c)]

[a)] *State Key Laboratory of Information Photonics and Optical Communications, Beijing University of Posts & Telecommunications, Beijing* 100876, *China*

[b)] *School of Information and Communication Engineering, Beijing University of Posts & Telecommunications, Beijing* 100876, *China*

[c)] *Institute of Infrared Optical Fibers & Sensors, Qinhuangdao* 066004, *China*

(Received 9 November 2011; revised manuscript received 14 December 2011)

Using a photonic crystal fiber with a zero dispersion wavelength of the fundamental mode at 780 nm designed and fabricated in our lab, the ultraviolet and mid-infrared continua are generated by cross-phase modulation between red-shift solitons and blue-shift dispersive waves. The dependences of continuum on the pump power and wavelength are investigated. With the pump working at 820 nm, when the pump power increases from 300 to 500 mW, the bandwidths of ultraviolet and mid-infrared continua change from 80 to 140 nm and 100 to 200 nm, respectively. The wavelength of ultraviolet continuum is below 246 nm, and the wavelength of mid-infrared continuum exceeds 2500 nm. Moreover, the influences of pump power on wavelength and conversion efficiency of different parts of continua are also demonstrated.

Keywords: photonic crystal fiber (PCF), ultraviolet and mid-infrared continuum, fundamental mode, soliton self-frequency shift

PACS: 42.70.Qs, 42.65.–k, 42.65.Sf, 78.47.nj **DOI:** 10.1088/1674-1056/21/7/074209

1. Introduction

Supercontinuum generation (SCG) in photonic crystal fiber (PCF)[1−3] has attracted extensive attention due to potential applications in pulse compression,[4] sensing techniques,[5] dispersion measurements,[6] all-optical telecommunication,[7,8] and source for optical coherence tomography with ultrahigh resolution in biological tissue.[9] The nonlinear phenomena of a supercontinuum are complicated and have been widely investigated.[10−12] The PCFs are particularly suited for SCG due to the tailored dispersion of guided modes[13,14] and strongly enhanced waveguide nonlinearity[15] by changing the fiber structure. Self-phase modulation (SPM), four-wave mixing (FWM),[16−18] Raman self-frequency shift (RSFS), and three-wave mixing (TWM) have been used to understand the supercontinuum generation. The zero-dispersion wavelength plays a very important role in the SCG. Usually, the wavelength of the ultrashort pump pulse is located in the anomalous dispersion region. It has been demonstrated that the generation and evolution of the infrared continuum are determined by higher-order soliton fission,[19] the visible component generation is caused mainly by the Raman soliton self-frequency shift (SSFS).[20,21] There are many reports on the near-infrared supercontinuum.[22−24] However, few PCF experiments have been conducted for the generation of ultraviolet and mid-infrared supercontinua.

Supercontinuum generation at 248 nm in high-pressure gas has been experimentally demonstrated,[25] but the bandwidth was only about 240 nm. The generation of supercontinua from 789 to 4870 nm

*Project supported by the National Key Basic Research Special Foundation of China (Grant Nos. 2010CB327605 and 2010CB328300), the Fundamental Research Funds for the Central Universities, China (Grant Nos. 2011RC0309 and 2011RC008), and the Specialized Research Fund for the Doctoral Program of Beijing University of Posts and Telecommunications, China (Grant No. CX201023).

†Corresponding author. E-mail: shenxiangwei03@gmail.com

was experimentally realized by using sub-centimeter segments of highly nonlinear Tellurite PCFs.[26] However, it does not cover the ultraviolet wavelength. Bartula *et al.*[27] experimentally demonstrated the generation of supercontinua covering 337–405 nm and 1500–3400 nm, but not covering 450–1500 nm.

In the present paper, mid-infrared and ultraviolet continua with bandwidth of above 2300 nm are generated by the cross-phase modulation between red-shift solitons and blue-shift dispersive waves in the fundamental mode of photonic crystal fiber with 120-fs Ti:sapphire laser. When the average pump power increases from 300 to 500 mW, the wavelengths of ultraviolet and mid-infrared waves can be less than 246 nm and greater than 2500 nm, respectively. The influence of other factors on experiment process are elementarily discussed.

2. PCF properties and experiment

The beam propagation method (BPM)[28] has been used to analyse the properties of group velocity dispersion of the PCF. The group velocity dispersion D can be expressed by

$$D = -\frac{2\pi c}{\lambda^2}\frac{\partial^2 \beta(\omega)}{\partial \omega^2},$$

where λ is the wavelength, w is the frequency, and β is the. Figure 1 shows the group velocity dispersion versus the wavelength for the fundamental mode of the PCF with zero dispersion wavelength at 780 nm. The cross-section structure of the PCF is shown in the inset of Fig. 1, where the core diameter is 2.0 μm and the relative air-hole size is 0.89 μm.

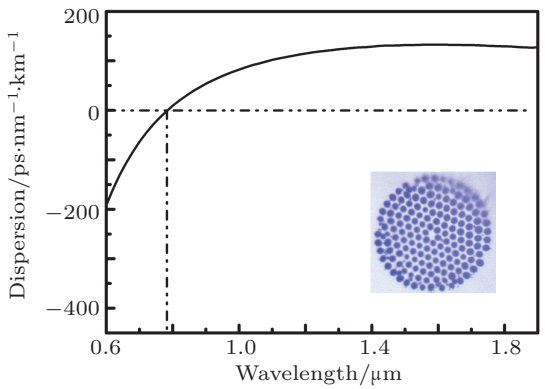

Fig. 1. (colour online) Group-velocity dispersion versus radiation wavelength for the fundamental mode of the PCF. The vertical dashed line corresponds to a zero dispersion wavelength of 780 nm and the inset indicates the cross section of PCF used in the experiment.

The configuration of the experimental setup is given by Fig. 2. The light source is a mode-locked Ti:sapphire laser, emitting a pulse train with a full width at half maximum (FWHM) of 120 fs at a repetition rate of 76 MHz. A variable attenuator is placed behind the laser to control the input energy, and an isolator is inserted to block the back reflection from the input tip of the fiber into the laser cavity. The 40× objective lenses each with a numerical aperture of 0.8 are used for adjusting input and output efficiency. CCD1 and CCD2 are used to observe the output mode field and check the coupling state of the input field, respectively. The fundamental mode can be selectively excited by using the offset pumping technique. After the beam passes through the first split-beam mirror, one part is coupled into a power meter to monitor the input average power, and the other part is coupled into a 50-cm-long PCF span. The coupling efficiency is above 70%. The transmission loss is 10 dB/m at 800 nm with the cutback method. The output spectra are monitored by two optical spectrum analyzers (OSA, Avaspec-256 and Avaspec-NIR-256) in the measurement scopes from 200 to 1100 nm and 900 to 2500 nm and with resolutions of 0.025 and 15 nm, respectively.

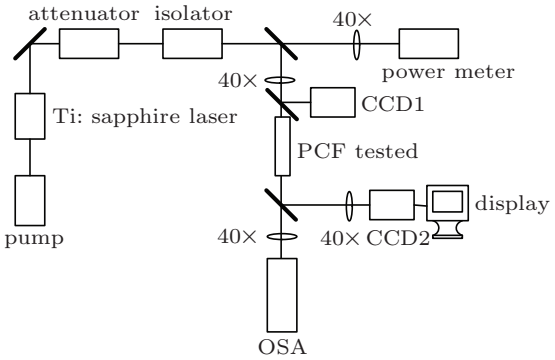

Fig. 2. Configuration of the experimental set up.

3. Results and discussion

The experimental condition and process are carefully optimized. The experiment is carried out by coupling femtosecond pulses with working wavelengths of 800 and 820 nm (lying in the anomalous dispersion region) and average power from 300 to 500 mW with the fundamental mode of PCF.

As shown in Fig. 3, when the pump wavelength is 800 nm, because of the interplay between the SPM and the negative dispersion, the fundamental solitons are formed. Due to the intra-pulse Raman scattering (IRS) (soliton self-frequency shift), this Raman-type

amplification appears, and the solitons constantly shift from 2000 to 2300 nm and the second solitons generated from the residual pump are observed in a range from 1100 to 1500 nm as the input pump power increases from 300 to 500 mW, as shown in Fig. 3(b). Simultaneously, the higher-order dispersion induces the instability of the first solitons, and the Cherenkov radiations (CRs) are generated in a range from 500 to 700 nm based on the phase matching between the red-shift solitons and the blue-shift waves. The ultraviolet waves are generated from 300 to 450 nm because of the XPM between the blue-shift waves and the solitons, as shown in Fig. 3(c). Since the soliton group velocity continuously decreases in the shift process, the XPM traps the CR, resulting in the equal group velocities of two waves. The pump power is greatly transferred into the solitons, CRs, and the ultra-blue waves, as shown in Fig. 3(a). Owing to the fact that the large index contrast between the diffraction and index-step guiding in PCF can be well controlled, the SPM and normal dispersion experienced by the femtosecond pulse broaden the CRs and the ultra-blue spectra. The absorption loss of the silica material at wavelength above 1800 nm will restrict the SSFS.

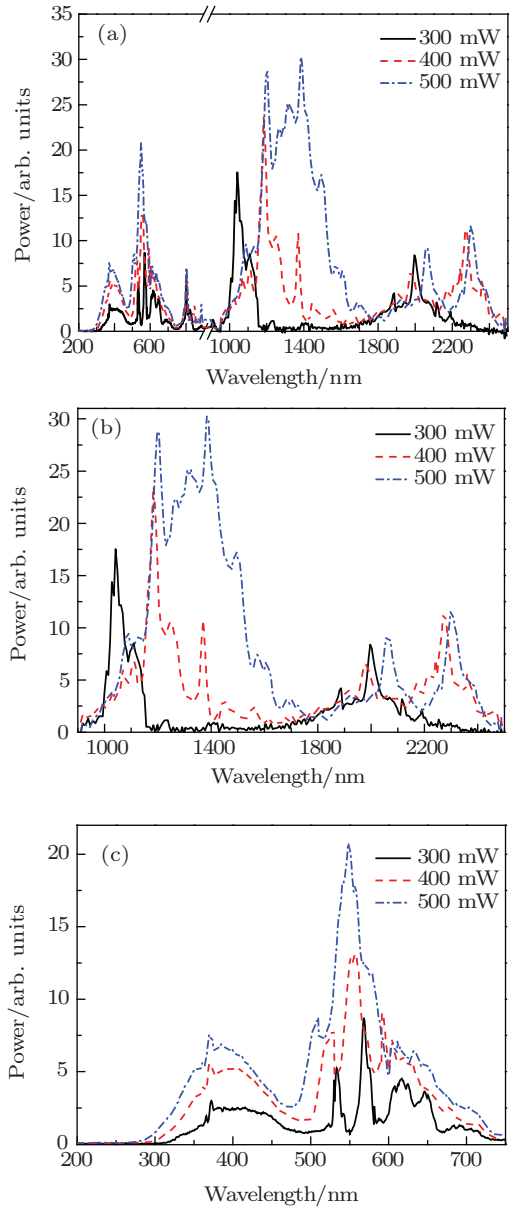

Fig. 3. (colour online) (a) Output spectrum power in a wavelength range from 200 to 2500 nm. Amplified output spectrum power of mid-infrared (b) and ultraviolet (c) components, with the pump pulse working at 800 nm and the input average power being 300, 400, and 500 mW.

At 820 nm, when the input power increases from 300 to 500 mW, the higher-order dispersion and IRS make the spectra spread out asymmetrically, as shown in Fig. 4(a). The continuum generation (CG) consists of four basic phases: when the femtosecond pulse is launched into the anomalous dispersion region, the SPM induces the broadening of the spectrum. The fission of a higher-order soliton into fundamental soliton components is due to the pulse self steep (SS) effect, higher-order dispersion and the propagation dynamics of the generated solitons and interaction between the soliton and the short-wavelength part of SC caused by SSFS, ultraviolet waves generated by the XPM between blue-shift wavelength and solitons. In the first phase, the SPM is viewed as the FWM of different frequency components belonging to a broad spectrum of radiation. Frequency components near the zero dispersion wavelength then serve as a pump for phase-matched FWM, which depletes the radiation spectrum around the zero dispersion wavelength and transfers the radiation energy to the regions of normal (< 780 nm) and anomalous (> 780 nm) dispersions. In the second phase, due to the simulated Raman scattering, the shorter-wavelength components are gradually converted into longer ones and the Raman spectral components are generated on the longer-wavelength side. In the third phase, on the one hand, the fundamental solitons constantly shift toward a longer wavelength due to the SSFS and this process is the Raman-type amplification at the expense of the depletion of its short-wavelength wing. On the other hand, the high-order dispersion induces the instabilities of these solitons and the dispersive waves referred to as CRs are generated at the shorter wavelengths

based on the phase matching between the red-shift solitons and blue-shift waves.[11] Because the soliton group velocity continuously decreases in the Raman shifting process, the XPM traps the dispersive waves, leading to blue shift up to wavelengths that make the group velocities of two waves equal. As the solitons progressively shift towards a longer wavelength, the dispersive waves experience SPM and are constantly widened.[24] In the fourth phase, due to the XPM between the blue-shift waves and the solitons, the ultraviolet and mid-infrared waves are generated. The intrinsic loss at mid-infrared and ultraviolet wavelengths and the SS effect are the main limiting factors. As seen in Fig. 4(a), CRs in a range from 450 to 550 nm are efficiently generated. The ultraviolet CG at 200 nm is shown in Fig. 4(b). The generated mid-infrared continuum can be over 2500 nm, limited by the measurement range of OSA. The observed far fields of CG at different wavelengths are shown in Fig. 4(d).

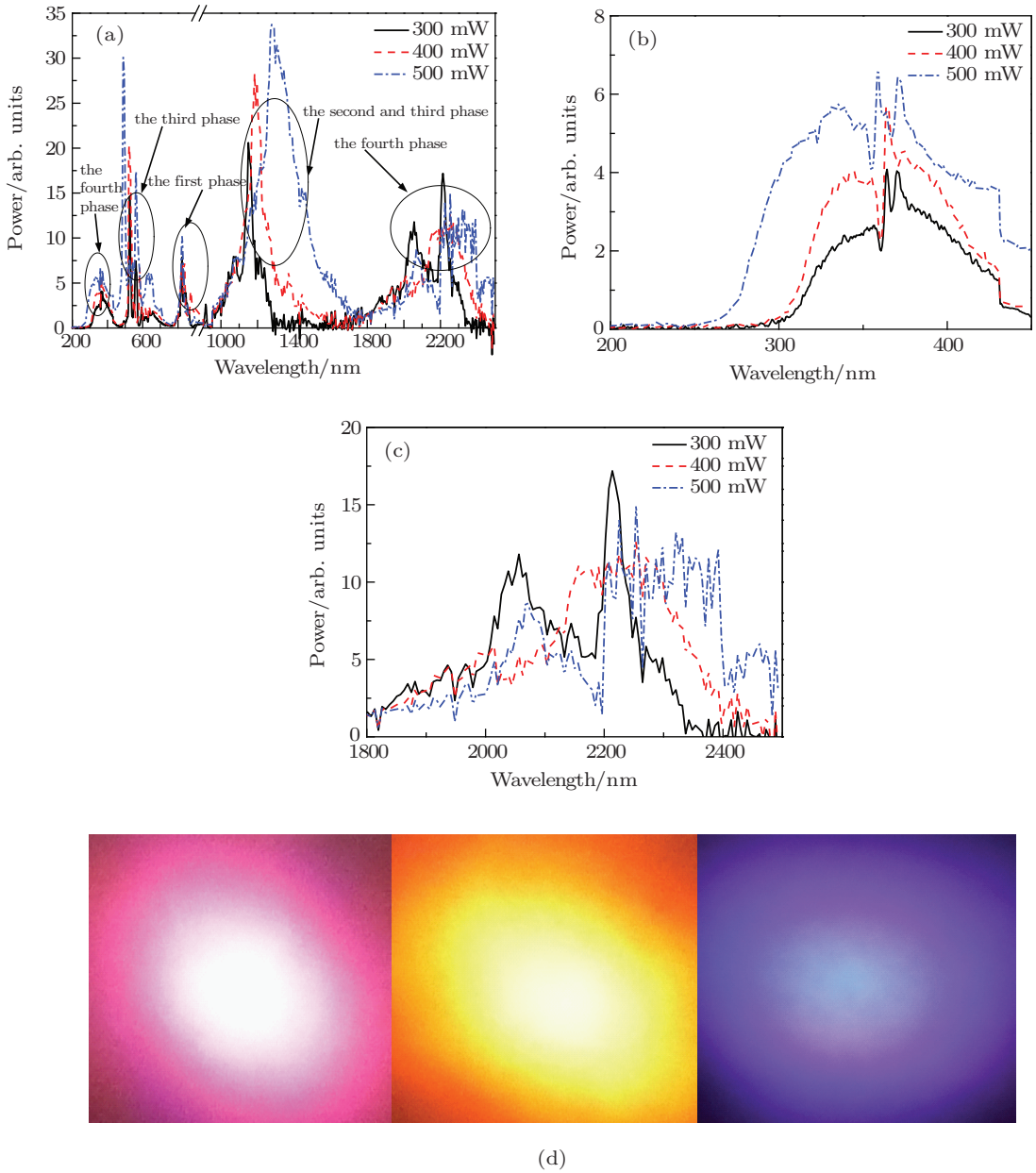

(d)

Fig. 4. (colour online) (a) Output spectrum powers in a wavelength range of 200–2500 nm. Amplified output spectrum powers of (b) mid-infrared and (c) ultraviolet components. (d) Corresponding far fields observed at different wavelengths (pink-white, orange-white, purple-blue). The pump pulse works at 820 nm and its input average power is 300, 400, and 500 mW, respectively.

As seen from Fig. 5(a), with the increase of the input power ($P_{\rm in}$), the output spectrum bandwidth (> 0) of the pump at 800 nm increases from 2034 to 2300 nm and then decreases from 2300 to 2276 nm. However, for pump pulse at 820 nm, the bandwidth increases from 1722 to 2300 nm. IRS, SPM, SS, XPM, and FWM lead to different results for the two pump pulses. In Fig. 5(b), $\eta_{\rm NI}$, $\eta_{\rm UV}$, $\eta_{\rm V}$, and $\eta_{\rm MI}$ are, respectively, the ratios of the output powers of the near-infrared waves, the ultraviolet waves, the visible waves, and the mid-infrared waves to the output power of the residual pump with the pump working at 820 nm. The $\eta_{\rm NI}$ is much higher than $\eta_{\rm UV}$, $\eta_{\rm V}$, and $\eta_{\rm MI}$. As the pump power increases from 300 to 400 mW, $\eta_{\rm NI}$, $\eta_{\rm UV}$, and $\eta_{\rm V}$ increase and $\eta_{\rm MI}$ decreases, because more pump power is transferred to the near-infrared waves, the ultraviolet waves, and the visible waves. When the pump power continues to increase from 400 to 500 mW, $\eta_{\rm NI}$, $\eta_{\rm UV}$, $\eta_{\rm V}$, and $\eta_{\rm MI}$ decrease. This is because with the increase of the pump power, the SPM, XPM, solitons, and CRs make the spectrum become broader and flatter. The peak powers of the near-infrared waves, the ultraviolet waves, the visible waves, and the mid-infrared waves decrease. More power is required to broaden the spectrum.

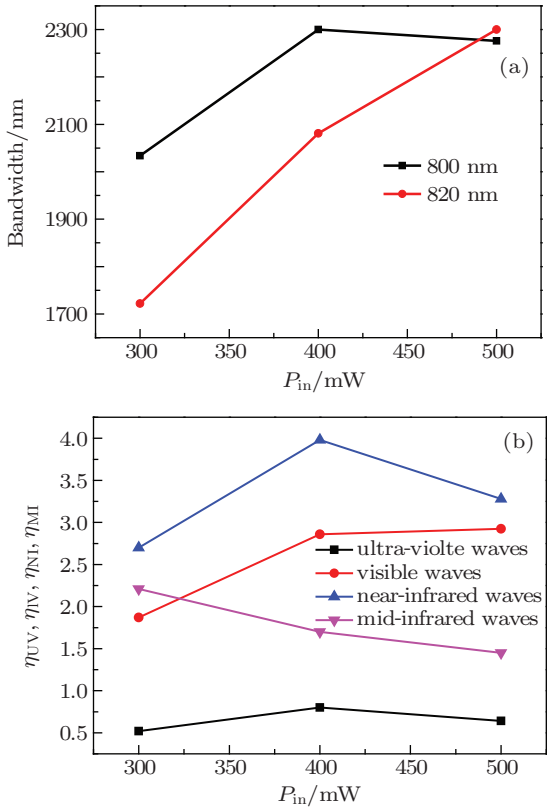

Fig. 5. (colour online) (a) Bandwidths (> 0) of pump pulses at 800 and 820 nm versus $P_{\rm in}$, and (b) conversion efficiencies of the near-infrared waves, the ultraviolet waves, the visible waves, and the mid-infrared waves versus $P_{\rm in}$.

4. Conclusions

With 120-fs pump pulses at 800 and 820 nm, mid-infrared and ultraviolet continua with a broadband of above 2300 nm are generated by cross-phase modulation between red-shift solitons and blue-shift dispersive waves in the fundamental mode of photonic crystal fiber. The dependences of the near-infrared waves, the ultraviolet waves, the visible waves, and the mid-infrared waves on the pump wavelength and power are investigated. The corresponding nonlinear-optical processes are analysed. The generated broadband continuum can be extensively applied to mid-infrared and ultraviolet photonics.

References

[1] Dudley J M, Genty G and Coen S 2006 *Rev. Mod. Phys.* **78** 1135
[2] Yuan J H, Sang X Z, Yu C X, Xin X J, Shen X W, Zhang J L, Zhou G Y, Li S G and Hou L T 2011 *Chin. Phys.* B **20** 054210
[3] Wang Y B, Xiong C L, Hou J, Lu Q S, Peng Y and Chen Z L 2011 *Acta Phys. Sin.* **60** 014201 (in Chinese)
[4] Chang G Q, Norris T B and Winful H G 2003 *Opt. Lett.* **28** 546
[5] Kelkar P V, Coppinger F, Bhushan A S and Jalali B 1999 *Electron. Lett.* **35** 1661
[6] Jasapara J, Her T H, Bise R, Windeler R and DiGiovanni D J 2003 *J. Opt. Soc. Am.* B **20** 1611
[7] Smirnov S V, Ania-Castanon J D, Ellingham T J, Kobtsev S M, Kukarin S and Turitsyn S K 2006 *Opt. Fiber Technol.* **12** 122
[8] Yan H F, Yu Z Y, Tian H D, Liu Y M and Han L H 2010 *Acta Phys. Sin.* **59** 3273 (in Chinese)
[9] Hartl J, Li X D, Chudoba C, Ghanta R K, Ko T H, Fujimoto J G, Ranka J K and Windeler R S 2001 *Opt. Lett.* **26** 608
[10] Kolesik M and Moloney J V 2004 *Phys. Rev.* E **70** 036604
[11] Liu B W, Hu M L, Fang X H, Li Y F and Chai L 2008 *Opt. Express* **16** 14987
[12] Agrawal G P 2001 *Nonlinear Fiber Optics* (3rd ed.) (New York: San Diego) pp. 469–475
[13] Nishizawa N and Goto T 2001 *IEEE J. Sel. Topics Quantum Electron.* **7** 518.
[14] Nishizawa N, Ito Y and Goto T 2002 *IEEE Photon. Technol. Lett.* **14** 983
[15] Knight J C 2003 *Nature* **424** 847
[16] Yuan J H, Sang X Z, Yu C X, Xin X J, Li S G, Zhou G Y and Hou L T 2010 *Chin. Phys.* B **19** 074218
[17] Yuan J H, Sang X Z, Yu C X, Li S G, Zhou G Y and Hou L T 2010 *IEEE J. Quantum Electron.* **46** 728
[18] Yuan J H, Sang X Z, Yu C X, Han Y, Zhou G Y, Li S G and Hou L T 2011 *J. Lightwave Technol.* **29** 2920

[19] Husakou A V and Herrmann J 2001 *Phys. Rev. Lett.* **87** 203901
[20] Tran T X and Biancalana F 2009 *Phys. Rev.* A **79** 065802
[21] Peng J H, Sokolov A V, Benabid F, Biancalana F, Light P S, Couny F and Roberts P J 2010 *Phys. Rev.* A **81** 031803(R)
[22] Bache M, Bang O, Zhou B B, Moses J and Wise F W 2010 *Phys. Rev.* A **82** 063806
[23] Baiz C R and Kubarych K J 2011 *Opt. Lett.* **36** 187
[24] Yuan J H, Sang X Z, Yu C X, Han Y, Zhou G Y, Li S G and Hou L T 2011 *IEEE Photon. Technol. Lett.* **13** 786
[25] Gosnell T R, Taylor A J and Greene D P 1990 *Opt. Lett.* **15** 130
[26] Domachuk P, Wolchover N A, Golomb M C and Wang A 2008 *Opt. Express* **16** 7161
[27] Bartula R J, Hagen C L, Walewski J W and Sanders S T 2006 *OSA/LACSEA* ThB2
[28] Hadley G R 1998 *J. Lightwave Technol.* **16** 134